CHLORINE-ISOTOPIC ANALYSIS OF APATITE IN AN OLIVINE-HOSTED MELT INCLUSION IN MAGNESIAN-SUITE TROCTOLITE 76535: FURTHER EVIDENCE OF A KREEP-RICH PARENTAL MAGMA? F. M. McCubbin[1] and J. J. Barnes[1,2]. [1]NASA Johnson Space Center, mailcode XI, 2101 E NASA Parkway, Houston, TX 77058, USA, [2]Lunar and Planetary Laboratory, University of Arizona, 1629 E University Blvd, Tucson, AZ 85721, USA (francis.m.mccubbin@nasa.gov)

Introduction: The lunar highlands magnesian suite rocks exhibit abundances of incompatible lithophile trace elements consistent with a substantial KREEP component **[1]**. Petrogenetic models describing the origin of magnesian-suite magmas implicate low-degree partial melting of a hybridized source that consisted of hot Mg-rich early lunar magma ocean cumulates that ascended to the base of the lunar crust during mantle overturn, anorthositic crust, and a minor KREEP-rich component **[1-3]**. In this model, the parental magmas of the magnesian suite samples are KREEP-rich. However, the magnesian suite samples are plutonic crustal rocks that underwent slow cooling, and previous studies have reported evidence that post-cumulate processes have affected the geochemistry of magnesian suite samples. In particular, previous studies reported that the KREEPy signatures of magnesian suite rocks could have been inherited through post-cumulate metasomatism by a magmatic liquid associated with the mafic conjugate liquid that likely formed when KREEP underwent silicate liquid immiscibility **[4-5]**. In addition, the most pristine magnesian suite troctolite, sample 76535, has symplectite assemblages that have been attributed to post-cumulate melt metasomatism **[6]**.

Although previous studies have made geochemical arguments as to why KREEP was a component in the source of the magnesian suite rather than a component that was added later **[7-10]**, many new insights into the geochemical and isotopic composition of KREEP have been determined, facilitating new avenues in which this question can be directly addressed with analysis of magnesian suite samples. Specifically, the Cl-isotopic composition of KREEP has been established to be about 25 to 30‰ based on the Cl-isotopic compositions of apatite measured in a wide range of lunar rock types **[e.g., 11-16**, Figure 1**]**. In the present study, we seek to compare the Cl-isotopic composition of intercumulus apatite and apatite within olivine-hosted melt inclusions in magnesian-suite troctolite 76535.

Methods: Apollo thin section 76535,56 was analyzed by nanoscale secondary ion mass spectrometry (NanoSIMS) in May of 2019. Both intercumulus apatite and apatite in a melt inclusion were analyzed. The Cl contents of the target apatites were accurately determined by electron probe microanalysis prior to NanoSIMS, therefore determination of Cl contents by NanoSIMS was not carried out. The sample and reference materials were coated with ~8 nm of carbon to aid charge compensation during analysis.

The Cameca NanoSIMS 50L at NASA's Johnson Space Center was used to measure the Cl isotopic composition of apatite in 76535. [$\delta^{37}Cl = ((^{37}Cl/^{35}Cl_{sample}/^{37}Cl/^{35}Cl_{standard}) - 1) \times 1000$, where SMOC = standard mean ocean chloride value]. A primary Cs^+ ion beam of ~5 pA was accelerated with a voltage of 8 kV. The NanoSIMS 50L ion probe was operated in multi-collection mode and the negative secondary ions of ^{13}C, $^{16}O^1H$, ^{18}O, ^{30}Si, ^{35}Cl, and ^{37}Cl were collected simultaneously in electron multipliers. The mass spectrometer was tuned to a mass resolving power of ~9000 (Cameca definition), which allowed isobaric interferences between $^{16}O^1H$ and ^{17}O to be resolved.

The incident ion beam of ~500 pA was rastered over ~400 μm^2 areas during ~10 minutes of pre-sputtering to clean the sample surface. The raster size was reduced to ~100 μm^2 during analysis. Isotope images were collected at 256×256 pixels with a dwell time of ~200 seconds per image plane. Between 20 and 40 image planes were collected depending on the heterogeneity of each location as determined during pre-sputtering and initial tuning using real time isotope imaging. Cracks were easily identified based on correlated highs of C, OH, and Cl ions in real time isotope imaging.

Two well-characterized terrestrial apatites were used in this work. Instrument mass fractionation (IMF) of $^{37}Cl/^{35}Cl$ ratio was between 1 and 5 ‰ during the analytical session as determined on repeat measurements of the standards.

Image processing was performed using software designed by S. Messenger at JSC. This software allowed regions of interest to be selected within each compiled image and the isotopic composition to be determined using the above IMF values.

Results: Intercumulus apatite and apatite within a single olivine-hosted melt inclusion were encountered in sample 76535,56. Backscattered electron (BSE) images of each apatite population is provided in Figure 2. The apatites were analyzed for major and minor elements by electro probe microanalysis, and the results have been reported previously **[6, 17]**. The apatite major and minor element compositions, including the F and Cl abundances of apatite between the two textural populations were indistinguishable. The Cl-isotopic

compositions of the intercumulus apatite is ~30-31 ± 1 ‰ (2σ), consistent with previous studies **[13]**, and the apatite within the olivine-hosted melt inclusion is ~28 ± 1 ‰ (2σ).

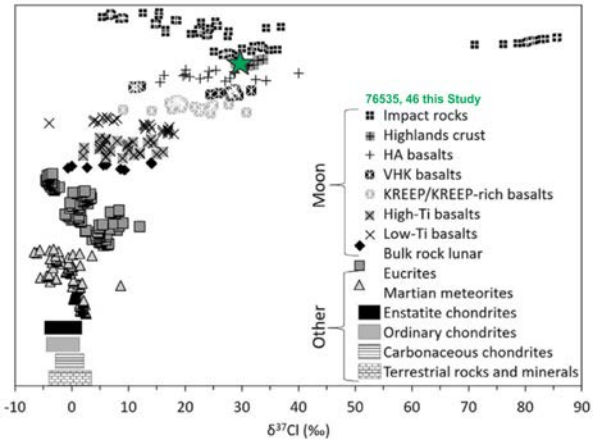

Figure 1. Cl-isotopic composition of lunar and other solar system materials as compiled by **[15]**. Green star represents data from this study. Figure adapted from **[15].**

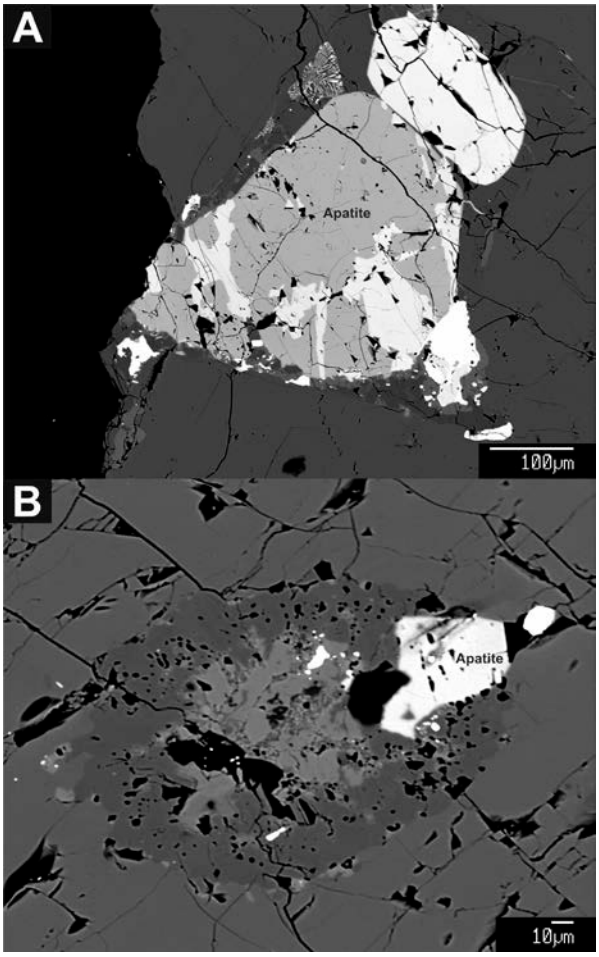

Figure 2. BSE images of apatite within A) intercumulus regions and B) olivine-hosted melt inclusions within lunar troctolite 76535.

Discussion: Within analytical uncertainties, apatite within the intercumulus regions of 76535 exhibit the same Cl-isotopic composition as apatites within olivine-hosted melt inclusions in 76535. This observation could indicate that 1) both the melt-inclusion apatite and intercumulus apatite have been reset to the same degree by secondary processes or 2) the Cl-isotopic compositions of the melt inclusion apatite and intercumulus apatite were inherited prior to the crystallization of the cumulate olivine and hence were likely an intrinsic feature of the parental liquids.

To address the first possibility, we draw an analogy to the martian sample Chassigny, which is a plutonic dunite that hosts apatite in olivine-hosted melt inclusions and intercumulus apatites. The two textural populations of apatite in Chassigny exhibit different Cl-isotopic compositions between the two populations consistent with a mantle Cl-isotopic reservoir recorded in the melt inclusion apatite and a crustal Cl-isotopic reservoir recorded in the intercumulus apatite **[18]**. Shearer et al. [18] demonstrated that Cl-isotopic compositions in slowly cooled plutonic samples can be preserved in apatites within olivine-hosted melt inclusions as long as the melt inclusion was not breached. Although there is no evidence of breaching apparent in our BSE images of the apatite-bearing melt inclusion in 76535, we only have access to a 2-D slice of the melt inclusion, so we cannot rule this possibility out entirely.

If the melt inclusion was not breached, the overlapping Cl-isotopic compositions in the two distinct textural populations in 76535 indicate that there may have been little-to-no modification of Cl isotopes during the long residence time of troctolite 76535 in the lunar crust. Furthermore, these data would indicate that the parental magmas for 76535 were KREEP-rich, consistent with the prevailing petrogenetic models for the origin of the magnesian suite samples **[1-3]**.

References: **[1]** Shearer et al. (2015) *Am Min*, 100, 294-325. **[2]** Shearer and Papike (2005) *GCA*, 69, 3445-3461. **[3]** Elardo et al. (2011) *GCA*, 75, 3024-3045. **[4]** Neal and Taylor (1989) *GCA*, 53, 529-541. **[5]** Neal and Taylor (1991) *GCA*, 55, 2965-2980. **[6]** Elardo et al. (2012) GCA, 87, 154-177 **[7]** Shearer et al., (2006) NVM, 60, 365-518. **[8]** Hess (1994) *JGR-Planets*, 99, 19083-19093. **[9]** McCallum and Schwartz (2001) *JGR-Planets*, 106, 27969-27983 **[10]** Prissel et al. (2016) *Am Min*, 101, 1624-1635. **[11]** Sharp et al. (2010) *Science*, 329, 1050-1053. **[12]** Boyce et al., 2015 *Science Advances*, 1, DOI: 10.1126/sciadv.1500380 **[13]** Barnes et al. (2015) *EPSL*, 447, 84-94. **[14]** Potts et al. (2018) *GCA*, 230, 46-59. **[15]** Barnes et al. (2019) *GCA*, 266, 144-162. **[16]** Wang et al. (2016) *Scientific Reports*, 9, doi.org/10.1038-/s41598-019-42224-8 **[17]** McCubbin et al. (2011) *GCA*, 75, 5073-5093. **[18]** Shearer et al. (2018) *GCA*, 234, 24-36.